Available online at www.sciencedirect.com

ScienceDirect

Procedia Structural Integrity 17 (2019) 98–104

Structural Integrity Procedia

www.elsevier.com/locate/procedia

ICSI 2019 The 3rd International Conference on Structural Integrity

Monitoring mass changes using nanoresonator sensors

Antonino Morassi[a]*, Michele Dilena[a], Marta Fedele Dell'Oste[a],

José Fernández-Sáez[b], Ramón Zaera[b]

[a]*University of Udine, Via Cotonificio 114,33100 Udine, Italy*
[b]*Universidad Carlos III de Madrid, Av. de la Universidad 30, 28911 Leganés, Madrid, Spain*

Abstract

Nanoresonators consisting in a one-dimensional vibrating structure have remarkable performance in detecting small adherent masses. The mass sensing principle is based on monitoring the resonant frequency shifts caused by unknown attached masses. In spite of its important application, few studies are available on this inverse problem. In this work, we have developed a distributed mass reconstruction method in an initially uniform nanobeam under bending vibration, by using finite eigenfrequency data belonging to one spectrum corresponding to supported end conditions. To avoid trivial non-uniqueness due to the symmetry of the initial configuration of the nanobeam, it is assumed that the mass variation has support contained in half of the axis interval. The nanobeam is modelled using the modified strain gradient elasticity accounting for size effects. The reconstruction is based on an iterative procedure, which takes advantage of a closed-form solution when the mass change is small, and shows to be convergent under this assumption. The identification method performs well even for not necessarily small mass changes, and in presence of errors on the data.

Peer-review under responsibility of the ICSI 2019 organizers.

Keywords: Inverse eigenvalue problems; nanobeams; mass identification; strain gradient theory; resonant frequencies.

* Corresponding author. Tel.: +39 0432 558739; fax: +39 0432 558700.
E-mail address: antonino.morassi@uniud.it

2452-3216
Peer-review under responsibility of the ICSI 2019 organizers.
10.1016/j.prostr.2019.08.014

1. Introduction

Nanosensors are gathering attention in the last decade due to the necessity of measuring physical and chemical properties in industrial or biological systems in the sub-micron scale, see, among other contributions, Arash and Wang (2013). One of the most representative examples of down-scaling in sensoring systems is the nanomechanical resonator, which typically consists in a one-dimensional vibrating structure with remarkable performance in detecting small adherent masses, see Rius and Pérez-Múrano (2016). The mass sensing principle for these systems is based on using the resonant frequency shifts caused by unknown additional mass attached on the surface of the sensor as data for the reconstruction of the mass variation. In spite of its important application, few studies are available on this inverse problem. The identification of a single point mass in a nanorod, modelled within the modified strain gradient theory to account for microstructure and size effects, see Lam et al. (2003) and Kong et al. (2009), was considered in Morassi et al. (2017) and Dilena et al. (2019a) by using minimal resonant frequency data.

The above cited works consider concentrated masses attached to the base system. However, the consideration of distributed added mass seems to be more realistic in real applications. In this respect, Hanay et al. (2015) proposed an inertial imaging method to determine the first N moments of the unknown mass distribution in terms of the frequency shifts in the first N resonant frequencies. Under the assumption of small global mass change, the obtained results using a classical clamped-clamped beam model to describe the transverse vibrations of a nanobeam were compared with experimental ones.

In this paper we have developed a method for the reconstruction of a distributed mass variation on an initially uniform nanobeam which uses the first N natural frequencies of the free bending vibration under supported end conditions. We refer to Barnes (1991) for a deep mathematical analysis of the main features of the inverse eigenvalue problems with finite data. Our method is based on an iterative procedure based on first-order Taylor expansion of the eigenvalues. The procedure determines an approximation of the unknown mass distribution by means of a generalized Fourier partial sum of order N, whose coefficients are calculated from the first N eigenvalues shifts. To avoid trivial non-uniqueness due to the symmetry of the initial configuration of the nanobeam, it is assumed that the mass variation has support contained in half of the axis interval. Moreover, the mass variation is supposed to be small with respect to the total mass of the initial nanobeam. As in previous works, the modified strain gradient theory has been used to account for the microstructure and size effects. An extended series of numerical examples shows that the method is efficient and gives good results with N less than 10 in case of smooth, e.g., continuous, mass variations. The determination of discontinuous coefficients exhibits no negligible oscillations near the discontinuity points, and requires more spectral data to obtain accurate reconstructions, typically N=15-20. Surprisingly enough, in spite of its local character, the identification method performs well even for not necessarily small mass changes.

2. Inverse problem and reconstruction method

The infinitesimal free vibration at radian frequency $\sqrt{\lambda}$ of the unperturbed uniform nanobeam, of length L and under supported end conditions, is governed by the eigenvalue problem (see Kong et al. (2009))

$$\begin{aligned} &Su^{IV} - Ku^{VI} = \lambda\rho_0 u, \qquad x \in (0, L), \\ &u(0) = 0, \;\; -Su''(0) + Ku^{IV}(0) = 0, \;\; u''(0) = 0, \\ &u(L) = 0, \;\; -Su''(L) + Ku^{IV}(L) = 0, \;\; u''(L) = 0, \end{aligned} \tag{1}$$

where λ is the eigenvalue and $u = u(x)$ is the associated eigenfunction. In equation (1), ρ_0=const, $\rho_0 > 0$, is the mass density per unit length, and S, K are positive constant coefficients which take into account both the mechanical properties and the length scale parameters of the nanobeam, see Agköz and Civalek (2011). The eigenpairs of (1) are $\lambda_n = \rho_0^{-1}(n\pi/L)^6\left(K + S(n\pi/L)^{-2}\right)$, $u_n(x) = (2/\rho_0 L)^{1/2}\sin(n\pi x/L)$, n≥1, where the eigenfunctions are normalized

with respect to the mass density ρ_0. Suppose that the mass density ρ_0 changes, and denote by $\rho(x)=\rho_0+r_\varepsilon(x)$ the mass density per unit length of the perturbed nanobeam. The mass variation $r_\varepsilon(x)$ is such that $(L^{-1}\int_0^L r_\varepsilon(x)dx)^{1/2}=\varepsilon\rho_0,\ r_\epsilon(x)\in L^\infty(0,L),\ 0<\rho^-\le\rho(x)\le\rho^+$ in [0,L], where $0<\varepsilon\le\varepsilon_\rho$, for a given small number ε_ρ, and ρ^-, ρ^+ are given constant. Moreover, we assume that support of the mass variation $r_\varepsilon(x)$ is a subset compactly contained in [0,L/2]. We denote by $(\lambda_n(\rho),u_n(x))_{n=1}^N$, n≥1, the nth eigenpair of the problem (1) with ρ_0 replaced by $\rho(x)$.

Our goal is the determination of an approximation to $\rho(x)$, or, equivalently, to $r_\varepsilon(x)$, using a finite amount of spectral data $\{\lambda_n(\rho)\}_{n=1}^N$, where N is a given integer. The proposed reconstruction method is based on an iterative procedure which, at every step, uses a linearized Taylor approximation of the eigenvalue in terms of the unknown mass variation. We first present the linearization in a neighborhood of the unperturbed nanobeam, next we shall introduce the iteration. A key mathematical tool is the explicit expression of the first order change of an eigenvalue with respect to the smallness parameter ε. With reference to the initial uniform nanobeam, we have

$$\delta\lambda_n=1-\frac{\lambda_n(\rho)}{\lambda_n}=\int_0^{L/2}r_\varepsilon(x)\Phi_n(x)dx,\quad\text{with}\quad\Phi_n(x)=(u_n(x))^2, \tag{2}$$

n=1,…,N. The family $\{\Phi_n(x)\}_{n=1}^\infty$ is a basis of the square integrable functions defined on the interval [0, L/2]. Therefore, we look for an N-dimensional approximation of the mass variation of the type

$$r_\varepsilon^{(0)}(x)=\sum_{k=1}^N\beta_k^{(0)}\Phi_k(x)\cdot\chi_{[0,L/2]}, \tag{3}$$

where $\chi_{[0,L/2]}$ is the characteristic function of the interval [0, L/2], and the numbers $\{\beta_k^{(0)}\}_{k=1}^N$ play the role of the Generalized Fourier Coefficients of the mass variation $r_\varepsilon^{(0)}(x)$. Replacing the expression (3) in (2), we obtain the NxN linear system

$$\delta\lambda_n=\sum_{k=1}^N A_{nk}\beta_k^{(0)},\ n=1,\dots,N,\ \text{with}\quad A_{nk}=\int_0^{L/2}\Phi_n(x)\Phi_k(x)dx,\ n,k=1,\dots,N. \tag{4}$$

A direct calculation shows that the linear system (4) admits a unique solution, which implies the following closed-form expression for the first order mass variation:

$$r_\varepsilon^{(0)}(x)=8\rho_0\sum_{k=1}^N\left(\frac{2N-1}{2N+1}\delta\lambda_k-\frac{2}{2N+1}\sum_{j=1,j\ne k}^N\delta\lambda_j\right)\sin^2\left(\frac{k\pi x}{L}\right)\cdot\chi_{[0,L/2]}, \tag{5}$$

see Dilena et al. (2019c). A better estimation of the mass variation $r_\varepsilon(x)$ can be obtained by iterating the above procedure. Let us denote by $\{\lambda_n^{EXP}\}_{n=1}^N$ the target values of the eigenvalues $\{\lambda_n(\rho)\}_{n=1}^N$. The mass coefficient $\rho(x)$ is estimated by the iteration $\rho^{(j+1)}(x)=\rho^{(j)}(x)+r^{(j)}(x)$, j≥0, where the increment $r^{(j)}(x)$ at the jth step is evaluated by solving a linear system analogous to (4), e.g., $\delta\lambda_n^{(j)}=\sum_{k=1}^N A_{nk}^{(j)}\beta_k^{(j)}$, n=1,…,N, where the coefficients $A_{nk}^{(j)}$ are

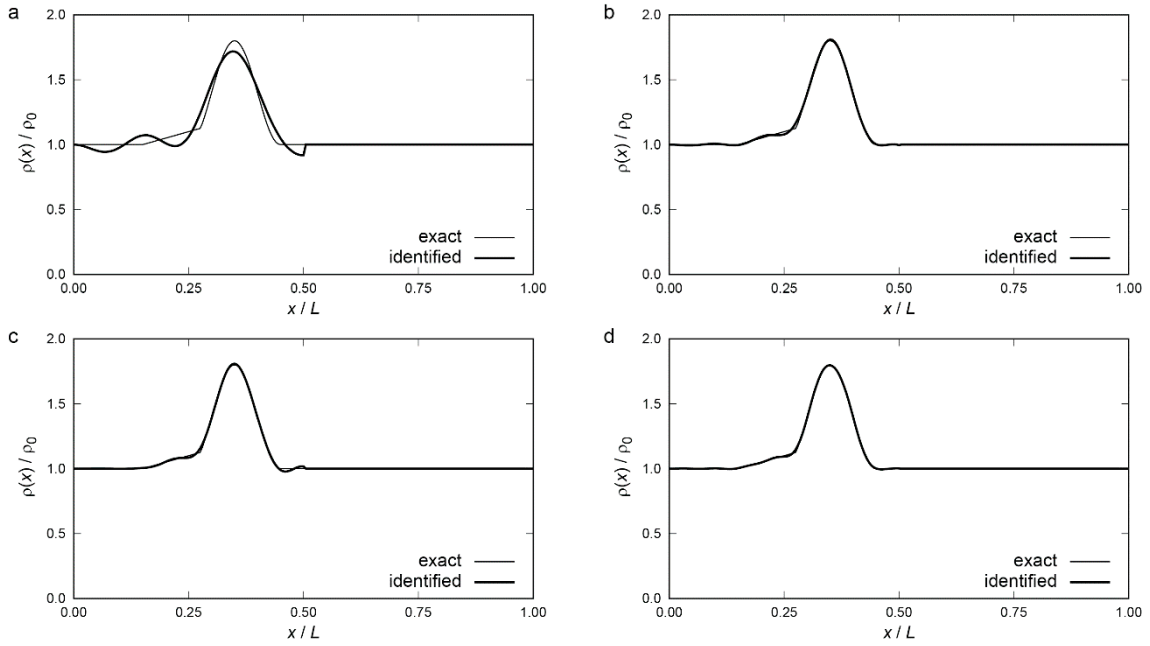

Fig. 1. Reconstruction of mass variation as in (6), with s/L=0.35, t=0.80, s_1/L=0.35, t_1=0.20. N=6 (a), N=9 (b), N=12 (c), N=15 (d).

defined as in (4), with the functions $\Phi_n(x)$ replaced by $\Phi_n^{(j)}(x) = \left(u_n\left(x;\rho^{(j)}(x)\right)\right)^2$, and $\delta\lambda_n^{(j)} = 1 - \lambda_n^{EXP} / \lambda_n\left(\rho^{(j)}\right)$. The iterations are stopped when the condition $e = N^{-1}\sqrt{\sum_{n=1}^{N}\left(\left(\lambda_n^{EXP} - \lambda_n\left(\rho^{(j)}\right)\right)/\lambda_n^{EXP}\right)^2} < \gamma$ is satisfied for a small given number γ. We refer to Dilena et al. (2019c) for a complete description of the procedure.

The convergence of the iterative procedure can be studied by adapting the arguments used in Dilena et al. (2019b), to study the analogous mass identification problem for nanobeams under axial vibration. Referring to this paper for more details, here we simply recall the main result in case of small and smooth mass variation. There exists a positive number ε_ρ, ε_ρ only depending on the a priori data of the inverse problem, such that if $\varepsilon \le \varepsilon_\rho$, then the iterative reconstruction procedure converges uniformly to a continuous function in [0,L/2] with the wished spectral properties, provided that $\sqrt{\sum_{n=1}^{N}\left(\delta\lambda_n^{(0)}\right)^2} < 1$.

3. Applications

In order to validate the reconstruction method, we developed a numerical code based on a finite element model of the nanobeam, with five-degree Hermite polynomial approximation of the transverse displacement of the nanobeam in each finite element. The spatial mesh consists of N_e equally spaced finite elements, and the mass coefficient is approximated by a continuous piecewise linear function. A preliminary series of tests suggests to assume a mesh with N_e=200 to manage cases with N up to 15, and to adopt N_e=400 for N=20, 25. The test specimen was selected as in Dilena et al. (2019a), with rectangular equivalent cross-section with thickness h=50 μm and width b=2h, and length L=20h. The three material length scale parameters l_i, i=0,1,2, were assumed to be equal to 17.6 μm, see Agköz and Civalek (2011). The mechanical and inertial properties of the material were chosen so that the coefficients S, K, ρ_0 are equal to $4.36\cdot10^{-9}$ Nm^2, $4.71\cdot10^{-19}$ Nm^4, $5\cdot10^{-6}$ kg/m, respectively.

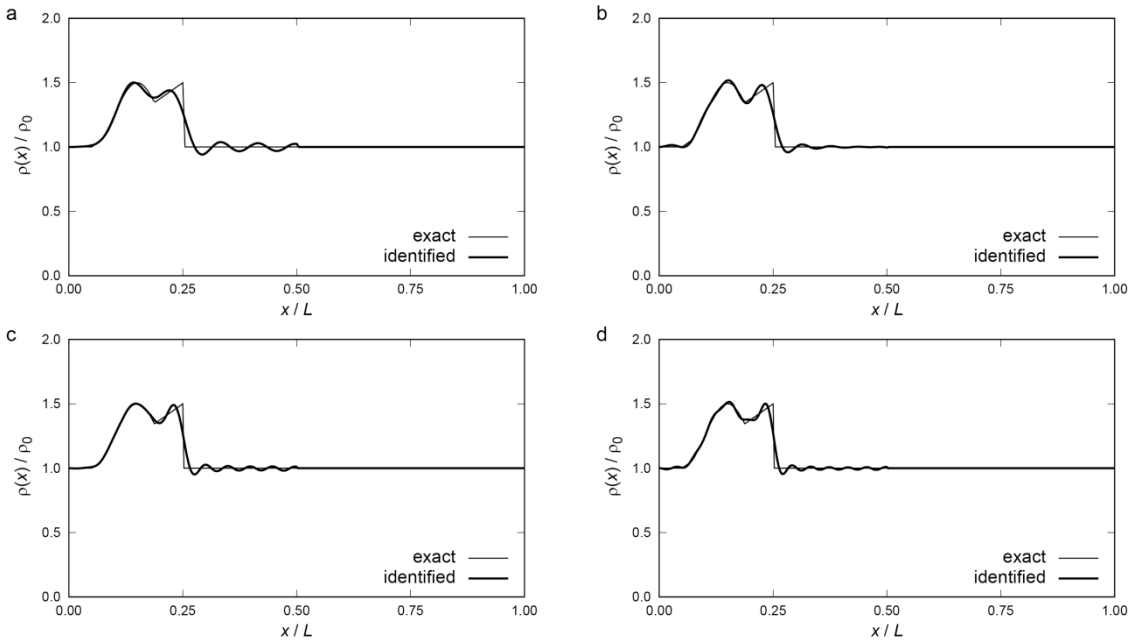

Fig. 2. Reconstruction of mass variation as in (6), with s/L=0.15, t=0.50, s_1/L=0.25, t_1=0.50. N=12 (a), N=15 (b), N=20 (c), N=25 (d).

We first consider free-error data, namely, only errors induced by the numerical approximation are included in the analysis. Among a large number of simulations, some representative results are presented here for the following mass density:

$$\rho(x)=\rho_0+\rho_0\cdot\max\left\{t\cos^2\left(\frac{\pi(x-s)}{c}\right)\chi_{\left[s-\frac{c}{2},s+\frac{c}{2}\right]},\ t_1\frac{x-(s_1-c_1)}{c_1}\chi_{[s_1-c_1,s_1]}\right\}, \tag{6}$$

where $[s-c/2,s+c/2]$ and $[s_1-c_1,s_1]$ belong to (0,L/2). Depending on the values of the parameters c, c_1, s, s_1, t, t_1, the definition (6) allows to obtain a large family of mass densities, including regular (e.g., continuous in [0, L/2]) or discontinuous (with jump discontinuity at x=s_1) functions. To simplify the presentation of the results, the condition c=c_1=0.2L has been chosen in this analysis.

The identification of regular mass variations leads to good results. Figure 1 shows a typical reconstruction. We see that the identified mass variation agrees well with the target function, and accuracy of reconstruction rapidly improves as N increases. Few iterations are sufficient to satisfy the convergence criterion with $\gamma=10^{-5}$, typically less than five iterations.

The determination of discontinuous mass coefficients is more problematic, since the pointwise reconstruction based on the family of regular functions $\{\Phi_n^{(j)}(x)\}_{n=1}^N$ is expected to fail near a jump discontinuity. Figures 2 and 3 show that spurious oscillations around the target coefficient occur near the discontinuity point, at x=s_1. These results, and also the results of other simulations performed for different discontinuous mass profiles, show that the maximum amplitude of the spurious oscillations is approximately proportional to the intensity of the jump, and the discrepancy decays far from the discontinuity. As a consequence, in presence of large jumps in the mass density, the induced oscillatory character of the identified coefficient may compromise the accuracy of the reconstruction in the whole, or at least in a significant portion of the interval [0, L/2]. Numerical results also show that a large number of first eigenfrequencies (typically N=20-25) and more iterations (up to 10-15) are needed to get reasonable accuracy in presence of large discontinuities. These cases has been developed with N_e=400 equally spaced finite elements. It

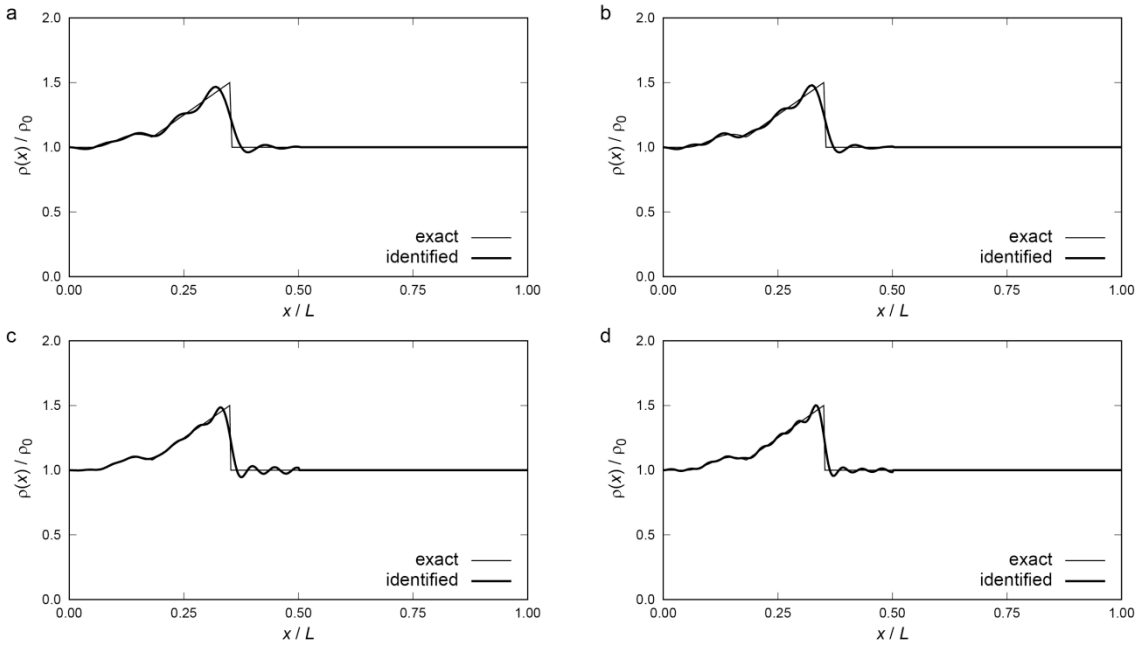

Fig. 3. Reconstruction of mass variation as in (6), with s/L=0.15, t=0.10, s_1/L=0.35, t_1=0.50. N=12 (a), N=15 (b), N=20 (c), N=25 (d).

should be noted that the undesired oscillations occurring near the discontinuities can be significantly reduced by using an optimization post-filtering based on a least squares-based minimization of the Euclidean norm between experimental and analytical eigenvalues. We refer to Dilena et al. (2019c) for more details.

To test the robustness of the method to errors on the data, the identification was performed by perturbing the target noise-free resonant frequencies corresponding to the eigenvalues $\left\{\lambda_n^{EXP}\right\}_{n=1}^{N}$ as $\sqrt{\lambda_n^{EXP-err}} = \sqrt{\lambda_n^{EXP}} + \tau_n$, where τ_n is a random Gaussian variable with vanishing mean and standard deviation σ such that $3\sigma = 2\pi\Pi$. Here, Π is the maximum admitted error. A selected, though representative, set of results are presented in Figure 4, for smooth and discontinuous mass coefficients, respectively. A thousand of simulations was performed for each case, with $\Pi = 100$ Hz and $\Pi = 200$ Hz. Each subfigure, besides the exact mass profile, contains three curves, namely the curve of the mean value and the two curves obtained by adding $\pm 3\sigma$ to the mean value. The three curves are almost indistinguishable for $\Pi = 100$ Hz, and the reconstruction is quite stable for $\Pi = 200$ Hz.

4. Conclusions

In this paper we have presented a reconstruction method for determining additional distributed mass on a supported nanobeam from finite number of natural frequencies and under the assumption that the mass is given on half of the nanosensor axis. To the authors' knowledge, this is the first quantitative study on the identification of distributed mass attached on nanobeams in bending vibration modelled within generalized continuum mechanics theories by using finite eigenvalue data. The extension of the method to the identification of general added mass distribution, e.g., not necessarily supported on half of the axis interval, is currently under investigation.

Acknowledgements

The authors from Universidad Carlos III de Madrid wish to acknowledge Ministerio de Economía y Competitividad de España for the financial support, under Grants DPI2014-57989-P and PGC2018-098218-B-I00.

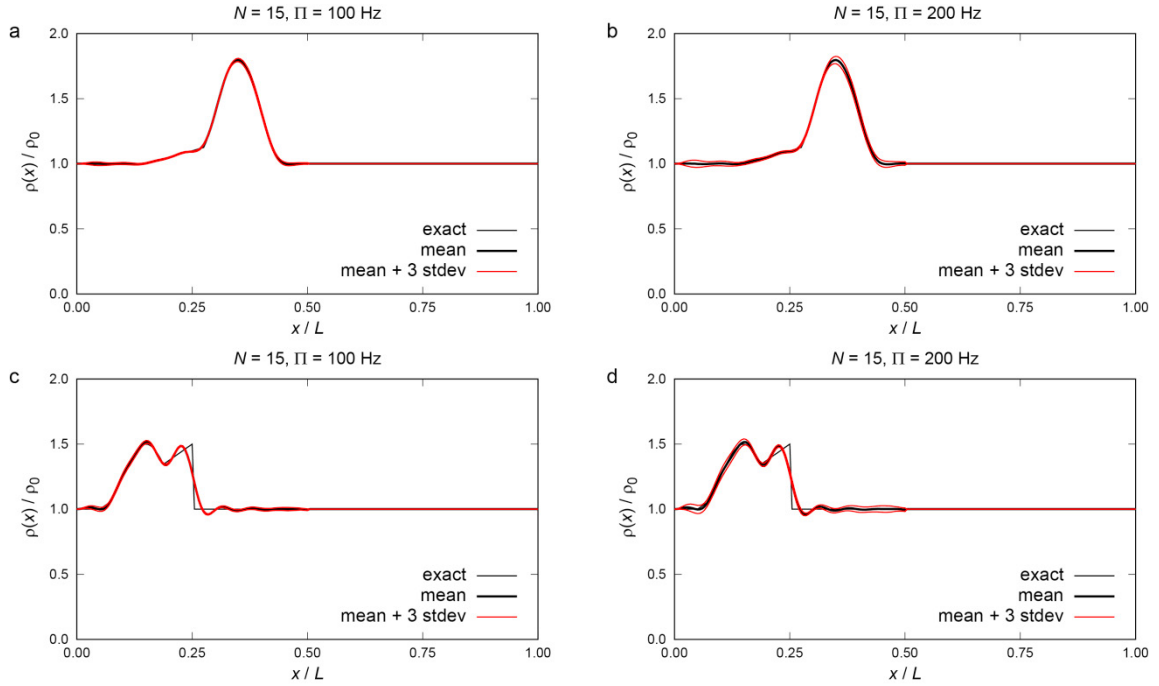

Fig. 4. Noise effects on identification. Upper row: mass variation as in (6), with s/L=0.35, t=0.80, s_l/L=0.35, t_l=0.20. Lower row: mass variation as in (6), with s/L=0.15, t=0.50, s_l/L=0.25, t_l=0.50.

The authors from University of Udine gratefully acknowledge the financial support of the National Research Project PRIN 2015TT JN95 'Identification and monitoring of complex structural systems'.

References

Akgöz, B., Civalek, Ő., 2011. Strain Gradient Elasticity and Modified Couple Stress Models for Buckling Analysis of Axially Micro-Scaled Beams. International Journal of Engineering Science 49, 1268–1280.

Arash, B., Wang, Q., 2013. Detection of Gas Atoms with Carbon Nanotubes. Scientific Reports 3, paper n. 1782.

Barnes, D.C., 1991. The Inverse Eigenvalue Problem with Finite Data. SIAM Journal on Mathematical Analysis 22, 732–753.

Dilena, M., Fedele Dell'Oste, M., Fernández-Sáez, J., Morassi, A., Zaera, R.., 2019a. Mass Detection in Nanobeams from Bending Resonant Frequency Shifts. Mechanical Systems and Signal Processing 116, 261–276.

Dilena, M., Fedele Dell'Oste, M., Fernández-Sáez, J., Morassi, A., Zaera, R.., 2019b. Recovering Added Mass in Nanoresonator Sensors from Finite Axial Eigenfrequency Data. Mechanical Systems and Signal Processing 130, 122– 151.

Dilena, M., Fedele Dell'Oste, M., Fernández-Sáez, J., Morassi, A., Zaera, R.., 2019c. Hearing Distributed Mass in Nanobeam Resonators, Preprint.

Hanay, M.S., Kelber, S.I., O'Connell, C.D., Mulvaney, P., Sader, J.E., Roukes, M.L., 2015. Inertial Imaging with Nanomechanical Systems. Nature Nanotechnology 10, 339–344.

Kong, S., Zhou, S., Nie, Z., Wang, K., 2009. Static and Dynamic Analysis of Micro-Beams Based on Strain Gradient Elasticity Theory. International Journal of Engineering Science 47, 487–498.

Lam, D.C.C., Yang, F., Chong, A.C.M., Wang, J., Tong, P., 2003. Experiments and Theory in Strain Gradient Elasticity. Journal of Mechanics and Physics of Solids 51, 1477–1508.

Morassi, A., Fernández-Sáez, J., Zaera, R., Loya, A., 2017. Resonator-Based Detection in Nanorods. Mechanical Systems and Signal Processing 93, 645–660.

Rius, G., Pérez-Múrano, F., 2016. Nanocantilever Beam Fabrication for CMOS Technology Integration, in *"Nanocantilever Beams: Modeling, Fabrication, and Applications"*. In: Voiculescu, I. and Zaghloul, M. (Eds.). CRC Press, Boca Raton, FL, pp. 544.